Desalination and Water Treatment
www.deswater.com
doi: 10.5004/dwt.2021.27227

225 (2021) 275–286
June

Separation of Fe(III) and Ni(II) in radioactive wastewater simulation liquid with a novel nuclear anion resin

Shuang Dai[a,b], Xinzhen Li[a,b], Yong Liu[a,b], Qi Cao[a,b], Yunming Chen[a,b,*]

[a]*Nuclear Power Institute of China, Chengdu, Sichuan 610065, P.R. China, Tel. 028-85904779; email: chenymnpic@126.com (Y. Chen), Tel. 028-85904026; email: 812007028@qq.com (S. Dai), Tel. 028-85904946; email: 361565556@qq.com (X. Li), Tel. 028-85904637; email: 634475250@qq.com (Y. Liu), Tel. 028-85904018; email: qicaonpic@163.com (Q. Cao)*
[b]*Sichuan Engineering Laboratory for Nuclear Facilities Decommissioning and Radwaste Management, Chengdu, Sichuan 610041, P.R. China*

Received 8 October 2020; Accepted 7 March 2021

ABSTRACT

In this work, to separate Fe(III) and Ni(II) in radioactive wastewater simulation solution, various parameters on adsorption and desorption efficiency were investigated by a novel nuclear anion resin. Considering the poor radiation resistance of separation materials, a commercial product nuclear grade ZG A NR 170 resin as an ion exchanger used in the process with excellent radiation resistance was utilized for the treatment of radioactive wastewater. A very good separation effect can reach by ZG A NR 170 resin. Through the ion exchange process, in the adsorption stage, more than 99% of iron can be adsorbed on the resin column, the $\beta_{(Ni/Fe)}$ of penetrating fluid can reach 1,223.93. In the desorption process, the desorption rate of iron is up to 98%, the $\beta_{(Fe/Ni)}$ of the desorption solution can reach 1,120.39. The volumetric mass-transfer coefficient of the static adsorption process can reach 0.032 s^{-1} and it shows excellent adsorption performance for five cycles under optimal conditions.

Keywords: Separation; Fe(III); Ni(II); Nuclear anion resin

1. Introduction

The radioactive wastewater was produced inevitably by the nuclear power plant, nuclear fuel pre-treatment, spent fuel post-treatment and radioisotope application process are receiving much attention from researchers because of the multiple hazards such as the emergence of disease, gene mutation and even chromosome aberration [1]. To treat these radioactive wastewaters, a large number of processing methods such as evaporation concentration [2], chemical precipitation [3], ion exchange [4] have been studied. As a post-processing technology, cement solidification is widely used in the treatment of radioactive wastewater because of its simple equipment and process, convenient operation and safety [5]. As the shield of radionuclide, the properties of cement solidified body, including compression resistance, frost resistance and leaching rate of radionuclide, need to be strictly controlled. Meanwhile, the activity of each nuclide in the leaching solution should be strictly controlled below the safety standard [6].

In the radioactive leaching solution, the main radionuclides were ^{3}H, ^{14}C, ^{55}Fe, ^{60}Co, ^{63}Ni, ^{90}Sr and ^{137}Cs. Of these radionuclides, the gamma emitters such as ^{60}Co, and ^{137}Cs Hou et al. [7] can be easily determined by gamma spectrometry. A rapid analytical method for ^{3}H, ^{14}C and ^{90}Sr in different types of samples also had been developed [8–10]. However, there was no efficient separation method for ^{55}Fe and ^{63}Ni. Both ^{63}Ni and ^{55}Fe are neutron activation products. ^{63}Ni is produced by two neutron reactions with Ni and Cu: $^{62}Ni(n,\gamma)$-^{63}Ni, $^{63}Cu(n,p)$-^{63}Ni and ^{55}Fe is produced by neutron activation reactions of two major stable

* Corresponding author.

The authors declare no competing financial interest.

iron isotopes: $^{54}Fe(n,\gamma)$-^{55}Fe and $^{56}Fe(n,2n)$-^{55}Fe. Due to poor energy resolution of beta spectroscopy and the high self-absorption of alpha particles in the samples, ^{55}Fe and ^{63}Ni in the radioactive leaching solution have to be completely separated as much as possible before the measurement.

To separate Fe(III) and Ni(II) in different types of samples, a large number of separation methods such as extraction, chemical precipitation, adsorption and ion exchange had been proposed (Table 1). Separation of Ni(II) and Fe(III), as well as other metals by hydroxide, was a fast method and its specific principle was that Fe^{3+} forms a $Fe(OH)_3$ precipitate, while Ni^{2+} formed a soluble $[Ni(NH_3)_4]^{2+}$ complex in NH_4OH solution. But only 80% of Ni(II) existed in the supernatant, and about 20% Ni was co-precipitated with $Fe(OH)_3$. A polystyrene microcapsules coated with Cyanex 272 (MC-Xs) was used to extract and separate the behavior of Cu(II), Zn(II), Fe(III) and Ni(II) in both batch, the results showed that almost 100% of stripping from loaded MC-Xs had been obtained using 0.1 and 0.5 M H_2SO_4 solution [28]. As an excellent extractant in the extraction of metal ions, bis(2-ethylhexyl) hydrogen phosphate (the order of extracting various metals is $Fe^{3+} > Zn^{2+} > Cu^{2+} > Co^{2+} > Ni^{2+}$) could separate various metal ions from different types of samples by adjusting the pH of the water phase to a certain extent. When the pH of the water phase was lower than 1, iron could be extracted almost completely, but nickel could hardly be extracted [29]. Meanwhile, some combined methods such as chemical precipitation–extraction, combined ion exchange, etc. were also used. In the chemical precipitation–extraction method, ^{55}Fe and ^{63}Ni were precipitated firstly in the form of hydroxide and subsequently purified by anion-exchange chromatography and dimethylglyoxime precipitation. After the purification, ^{55}Fe and ^{63}Ni were determined by a liquid scintillation calculator [30]. Although precipitation, ion exchange and conventional extraction have been widely used to separate ^{55}Fe and ^{63}Ni, they could meet the needs of measurement. There are still some shortcomings in the above methods, mainly in the following aspects:

- Separation process is complex and time-consuming;
- Complete and effective separation of interfering radionuclides cannot be achieved.

In view of the above disadvantages, a large number of new functional materials and separation technologies have been used to separate metal elements, including various types of extraction resins, new extractants, ionic liquids, organic metal framework materials or devices [31–38]. A novel extraction chromatographic resin based on diisobutyl ketone had been developed for the isolation of ^{55}Fe. This material was used in conjunction with a dimethylglyoxime-based resin for the sequential separation of ^{55}Fe and ^{63}Ni and isolation of these radionuclides from associated contaminants [39]. A new technique of liquid–liquid microextraction was also used to improve the separation efficiency due to some unique advantages such as high surface to volume ratio etc. Three types of microchannels slit interdigital micromixer, coiled flow inverter and 3D converging-diverging microreactor, respectively were applied for the extraction and separation of cobalt and nickel, and the effects of different processing and structural parameters were also studied. Compared with conventional macro-scale reactors and unstructured straight microchannel reactors, in the above three structured microreactors, the higher extraction ratio, separation factor and mass transfer performances had been achieved to shorter residence time [40]. Although these specific new materials or devices can simplify the separation process and realize the effective separation of interfering radionuclides, some thorny problems also arise such as the high price of these commercialized functional materials and the amount of potentially processed samples will be limited. Therefore, a fast and economical method to separate nuclides is expected to be found.

In this work, a modified separation method for Fe(III) and Ni(II) in radioactive wastewater simulation liquid was tested. Various parameters such as the acidity of the feed solution, washing liquid, and desorption solution on separation of Fe(III) and Ni(II) were investigated comprehensively by using a novel nuclear anion resin to develop an accurate, economic, sensitive and simple method for the separation of Ni(II) and Fe(III) in radioactive wastewater simulation liquid.

2. Experimental section

2.1. Materials and equipment

Hydrochloric acid (CAS: 7647-01-0), nitric acid (CAS: 7697-37-2), anhydrous ethanol (CAS: 64-17-5) and sodium hydroxide (CAS: 1310-73-2) were purchased from Chengdu Chemical Reagent Factory (purity level: GR). Both hydrochloric acid and nitric acid were purified by distillation. Nuclear anion exchange resin (Model: ZG A NR 170) was obtained from Zhejiang Zhenguang Industry Co., Ltd., (China). Iron standard solution (CAS: 7439-89-6, 1,000 mg/L) and nickel standard solution (CAS: 7440-02-0, 1,000 mg/L) were purchased from the National Center of Analysis and Testing for Nonferrous Metals and Electronic Materials (NCATN) (P.R. China). Ultrapure water was produced by ultrapure water equipment which was purchased from Beijing PUXI General Instrument Co., Ltd., (GWB-1E, P.R. China). Wastewater simulation liquid was used as the treatment object, and simulation solution with different acidity was prepared by Fe(III) and Ni(II) standard solution. The different acidity of the feed solution, washing liquid, and desorption solution was also prepared. The conditions of the experimental systems were shown in Table 2.

2.2. Pretreatment of nuclear anion resin

The ZG A NR 170 resin which its properties are shown in Table 3 should be pretreated before first use and the specific steps were as follows:

- *Step one*: After resin loading, the washing liquid including ultrapure water and ethanol washed the resin at a flow rate of about 10 mL/min to remove the organic, suspended impurities, mechanical impurities, fine resin and bubbles. The resin was washed by ultrapure water and ethanol alternately for 5 times, each time lasting for 15 min;

Table 1
Comparison of different methods for separation of Fe(III) and Ni(II)

References	Separation method	Separation objects
Gomez et al. [11]	Rosin as extractant, toluene as diluent	Aqueous solutions of Co(II), Ni(II), Cr(III), Fe(III) and Mn(II)
Sun et al. [12]	Modified polymer affinity liquid–solid extractant	Aqueous solutions of Cu(II), Zn(II), Co(II) and Ni(II)
Berber and Alpdogan [13]	Functionalized polymer microspheres prior	Trace Al(III), Fe(II), Co(II), Cu(II), Cd(II) and Pb(II) ions in beverages
Fernandes et al. [14]	Hydrochloric acid leaching, solvent extraction and precipitation	Ni(II), Co(II) and lanthanides from spent Ni–MH batteries
Shih et al. [15]	Fered-Fenton and chemical precipitation	Electroless Ni(II) plating wastewater
Tokalıoğlu and Daşdelen [16]	Co-precipitation with Cu(II)-4-(2-pyridylazo)-resorcinol	Fe(III) and Ni(II) in water and food samples
Pinto et al. [17]	Chemical precipitation	Ni(II) from an EDTA leachate of spent hydrodesulphurization catalyst
Yamakawa et al. [18]	Thermal ionization mass spectrometry separation	Cr(III), Fe(III), Ni(II), Zn(II) and Cu(II) in terrestrial and extraterrestrial materials
Liu et al. [19]	Oxidation leaching–chemical precipitation	Mo and Ni from spent acrylonitrile catalysts
Zhao et al. [20]	Adsorption by dialdehyde o-phenylenediamine starch	Aqueous solutions of Ni(II) ions
Shukla et al. [21]	Adsorption by modified coir fibres	Aqueous solutions of Ni(II), Zn(II) and Fe(II)
Bhattacharyya and Gupta [22]	Adsorption by ZrO–kaolinite and ZrO–montmorillonite	Fe(III), Co(II) and Ni(II) in aqueous medium
Qureshi et al. [23]	Ion-exchange by stannic arsenates	Fe(III) from Ni(II), [CO](II) Mn(II) and Al(III) in aqueous medium
Choi et al. [24]	Ion-exchange by AG MP-1	Stainless steel waste samples of ^{99}Tc, ^{90}Sr, ^{59}Fe, ^{63}Ni, ^{55}Fe and ^{94}Nb
Muslu and Gülfen [25]	Thiourea-formaldehyde resin	Selective separation Pd(II) from Fe(III), Co(II), Ni(II) and Cu(II) ions
Juang and Wang [26]	Cation-exchange by water–soluble complexing agents	Co(II), Ni(II) from aqueous solutions
Ahamed et al. [27]	Cation-exchange terpolymer involving 2-amino-6-nitrobenzothiazole-ethylenediamine-formaldehyde	Fe(III), Co(II), Ni(II), Cu(II), Zn(II) and Pb(II) from aqueous solutions

- *Step two*: The ZG A NR 170 resin was soaked for 24 h in 10% salt solution, and then rinsed to neutral with ultrapure water;
- *Step three*: The ZG A NR 170 resin was soaked for 8 h with 3% sodium hydroxide and hydrochloric acid solution and then washed it to neutral with ultrapure water.

2.3. Experimental procedure and analysis

A schematic diagram of the experimental setup is shown in Fig. 1. The experimental process included three processes: adsorption process, washing process and desorption process. Feed solution, washing liquid and desorption solution were individually fed into the resin column by a dual-channel peristaltic pump (BT100-2J, Longer Precision Pump Co., Ltd., China). The mass transfer also took place quickly in the resin column during this process. After ion exchange, the solution flowing through the resin column will be collected and analyzed for Fe(III) and Ni(II) concentration by inductively coupled plasma spectrometer (ICP) (IRIS-HR-DUO, Thermo Jarrell Ash, America). To improve the accuracy of the experiment, peristaltic pumps were calibrated before starting the experiments. All measuring instruments were regularly verified by the National Institute of Measurement and Testing Technology (Chengdu, Sichuan, P.R. China).

3. Results and discussion

3.1. Adsorption dynamics on nuclear anion resin

In general, the adsorption process consists: (1) liquid membrane transfer; (2) solid membrane transfer; (3) the reaction of the adsorption on the adsorption level of three steps.

The liquid membrane transfer coefficient can be described as follows:

$$\rho_b \frac{dq}{dt} = K_f^1 \cdot a_v \left(C - C_1\right) \tag{1}$$

Table 2
Conditions of the experimental systems

Experimental system	Feed solution (mol/L)				Washing liquid (mol/L)				Desorption solution (mol/L)				
Hydrogen chloride concentration (mol/L)	2	4	6	8	2	4	6	8	0.05	0.10	0.25	0.5	1.0
Concentration of iron and nickel (ppm)	$C_{(Fe)}$ = 6.63 ppm $C_{(Ni)}$ = 6.01 ppm				None				None				

The solid film transfer coefficient can be described as follows:

$$\rho_b \frac{dq}{dt} = K_s^1 \cdot \alpha_v \left(q_1 - q\right) \tag{2}$$

The total mass transfer coefficient can be described as follows:

$$\rho_b \frac{dq}{dt} = K_f \cdot \alpha_v \left(C - C^*\right) = K_s \cdot \alpha_v \left(q^* - q\right) \tag{3}$$

The material balance equation of the adsorption process can be defined as follows:

$$q = \frac{\left(C_0 - C\right)V}{m} \tag{4}$$

Putting the above formula into Eq. (3) can be turned into Eq. (5) as follows:

$$-\frac{dC}{dt} = \frac{mk_a}{\rho_b V}\left(C - C_e\right) \tag{5}$$

The following expression is obtained with integral treatment on Eq. (5):

$$\log\frac{C_0 - C_e}{C - C_e} = \frac{m_{0a}}{2.303\rho_b V}t \tag{6}$$

In order to obtain the volumetric mass-transfer coefficient, the adsorption experiment and desorption experiment were carried out. The relationship between the concentration of Fe(III) and Ni(II) in the adsorption and desorption process and time is shown in Figs. 2 and 3.

The resin quality, water sample volume and apparent density remain constant, the relationship of $\log[(C_0 - C_e)/C - C_e]$ and adsorption time is shown in Fig. 4. The slope of the equation is 0.0172. The volumetric mass transfer coefficient can be calculated as 0.032 s^{-1}.

3.2. Effect of acidity of feed solution on adsorption

The relationship between the concentration of Fe(III) and Ni(II) in the effluent volume is shown in Fig. 5. At high acidity, the concentration of Fe(III) in the effluent was maintained at a low level, but with the decrease of hydrochloric acid concentration, the concentration of Fe(III) began to increase gradually. However, the concentration of Ni(II) in the effluent was not affected by the concentration of hydrochloric acid.

Table 3
Properties of the ZG A NR 170 resin

Resin name	Nuclear strong basic anion resin
Model	ZG A NR 170
Functional group	$-N(CH_3)_3OH$
Bulk density, g/mL	0.685
Particle size range, mm	>3.8
Maximum service temperature, °C	60
Quality full exchange capacity, mmol/g	0.40–1.20

It is well known that Fe(III) forms a series of complexes in acidic chloride media with a distinct distribution of the species Fe^{3+}, $FeCl^{2+}$, $FeCl_2^+$, $FeCl_3$, $[FeCl_4]^-$ and $[FeCl_6]^{3-}$ depending on the HCl concentration [31]. Under different acidity conditions, the morphology of Fe(III) ions can vary greatly. At low acidity, the predominant species is $FeCl^{2+}$, $FeCl_2^+$ or $FeCl_3$, at a molarity of 6, the predominant species is $[FeCl_4]^-$, as the acidity continues to increase, Fe(III) will coordinate with hexachloroianoids to form $[FeCl_6]^{3-}$. When the concentration of hydrogen ion in the feed solution was 6–8 mol/L, it exists in the form of $[FeCl_4]^-$ or $[FeCl_6]^{3-}$, and can be adsorbed by ion exchange with anion resin. However, Ni(II) ions can only exist in the form of cations (Ni^{2+}, $NiCl^+$) at any acidity. This explains why the lower the acidity of the feed solution, the worse the adsorption effect of iron(III), but no effect on nickel(II) adsorption. This phenomenon can be explained by the following equations:

$$Fe^{3+} + 4Cl^- = \left[FeCl_4\right]^- \tag{7}$$

$$Fe^{3+} + 6Cl^- = \left[FeCl_6\right]^{3-} \tag{8}$$

$$R - N\left(CH_3\right)_3 Cl + \left[FeCl_4\right]^- = R - N\left(CH_3\right)_3\left[FeCl_4\right] + Cl^- \tag{9}$$

$$3\left[R - N\left(CH_3\right)_3 Cl\right] + \left[FeCl_6\right]^{3-} = \left[R - N\left(CH_3\right)_3\right]_3\left[FeCl_6\right] + 3Cl^- \tag{10}$$

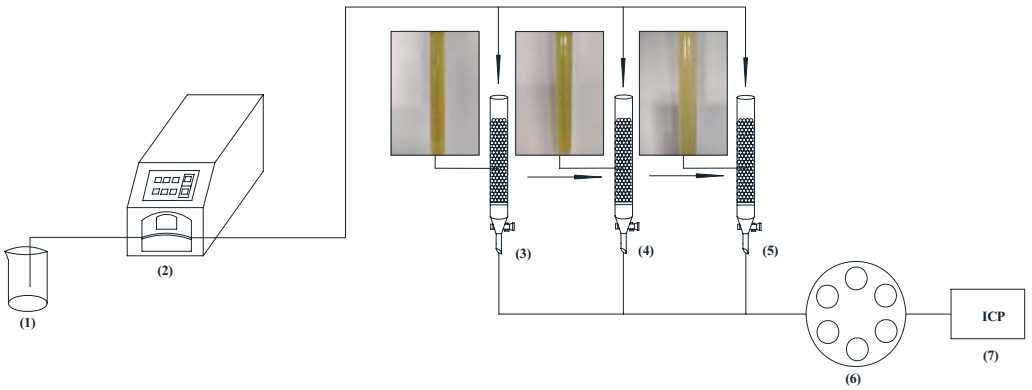

Fig. 1. Schematic diagram of the experimental setup used in the present experiments: (1) feed solution storage, (2) dual-channel peristaltic pump, (3) adsorption process, (4) washing process, (5) desorption process, (6) sampling disc, and (7) inductively coupled plasma spectrometer (ICP).

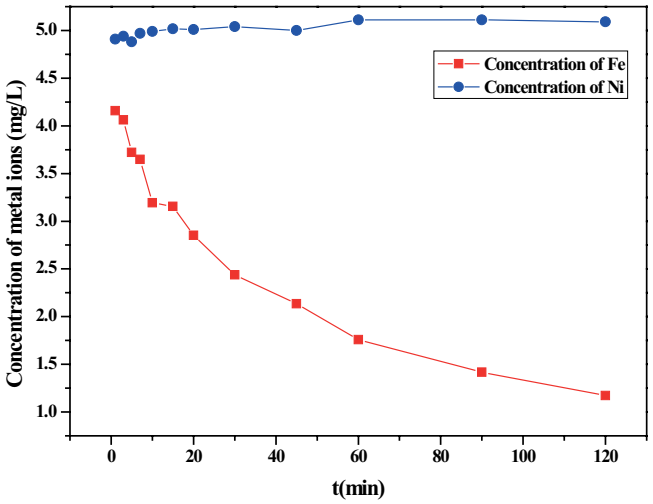

Fig. 2. The trend of iron and nickel concentration with time on adsorption process. Condition: T = 20°C; t = 120 min; R = 150 r/min; $V_{(\text{feed solution})}$ = 250 mL.

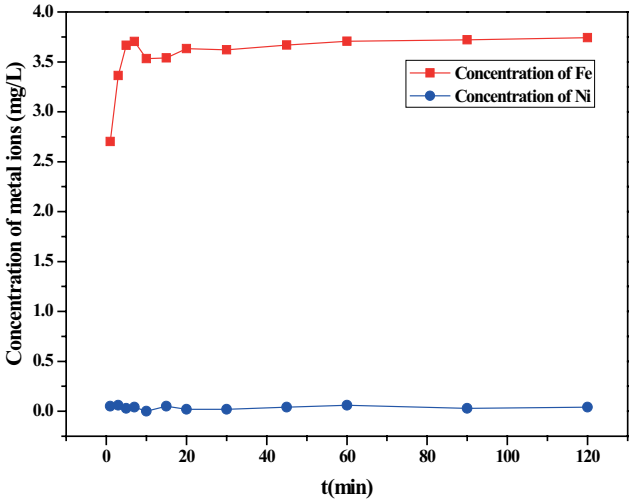

Fig. 3. The trend of iron and nickel concentration with time on desorption process. Condition: T = 20°C; t = 120 min; R = 150 r/min; $V_{(\text{feed solution})}$ = 250 mL.

The cumulative adsorption rate of Fe(III) and Ni(II) with effluent volume are shown in Fig. 6, the cumulative adsorption rate of Fe(III) was positively proportional to the accumulation of effluent volume and the acidity of feed solution. Obviously, with the increase of acidity from 2 to 8 mol/L, the cumulative adsorption rate of iron increased from 60% to 99%. Under this condition, a considerable part of iron which the form of iron in feed solution is $FeCl^{2+}$, $FeCl_2^+$ or $FeCl_3$ turn to $[FeCl_4]^-$ or $[FeCl_6]^{3-}$. This explained why the higher the acidity, the higher the adsorption rate. The cumulative adsorption rate of Ni(II) was proportional to effluent volume but inversely proportional to the acidity of feed solution. When the concentration of hydrochloric acid was higher than 4 mol/L, the adsorption rate of nickel was maintained at 18%, and the acidity had no effect on the absorption of resin of nickel. The adsorption of nickel was a simple physical adsorption process, which did not involved ion exchange. The adsorption rate of nickel increased significantly as the concentration of

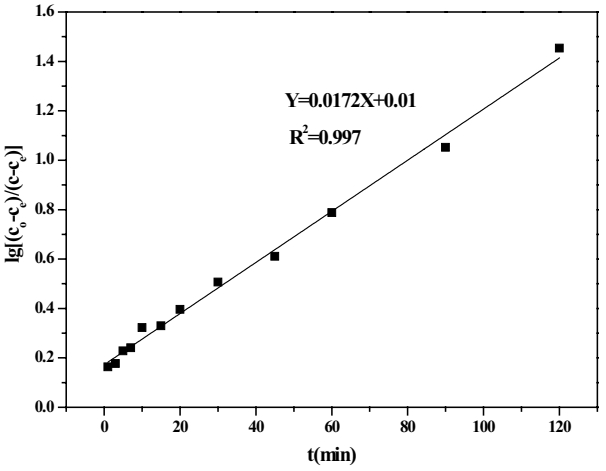

Fig. 4. The relationship between $\log[(C_0 - C_e)/C - C_e]$ and adsorption time. Condition: T = 20°C; t = 120 min; R = 150 rpm; $V_{(\text{feed solution})}$ = 250 mL.

hydrochloric acid decreased to 2 mol/L. This was because when the acidity decreased, the adsorption rate of iron decreased and the physical adsorption of nickel increased.

Fig. 7 shows the separation coefficients of Ni(II) and Fe(III) at different acidity of feed solution. It can be seen from Fig. 7 that the separation of Ni(II) and Fe(III) can be carried out by controlling the acidity of the feed solution. The separation coefficient of $\beta_{(Ni/Fe)}$ increased with the increase of the acidity. When the hydrochloric acid concentration increases from 2 to 8 mol/L, the $\beta_{(Ni/Fe)}$ increases from 1.21 to 1,223.93. Which indicated that it is easy to separate Fe(III) and Ni(III) by controlling the acidity of the feed solution. Therefore, the acidity of 8 mol/L was selected as optimum.

3.3. Effect of acidity of washing solution

The trend of Fe(III) and Ni(II) concentration with the volume of the washing solution is shown in Fig. 8. When the acidity of the washing solution was 6 mol/L or higher, only a very small amount of iron was presented in the washing solution. This is because most of the iron is firmly adsorbed on the resin column. At the same time, part of nickel(II) is adsorbed on the resin column by physical adsorption, especially in the earlier stage of the washing process. With the decrease of acidity, the amount of iron washed gradually increases. Fig. 9 shows the variation of cumulative washing rate with the effluent volume of the washing solution. Obviously, the cumulative washing rate of iron(III) and nickel(II) increased with the increase of washing solution volume. With the decrease of acidity, the cumulative washing rate of iron(III) and nickel(II) showed the opposite trend. When the volume of leaching solution is 20 mL, the leaching rate of iron increased from 1% to 18%, while that of nickel decreased from 18% to 6%. The reasons for this trend are detailed in Section 3.2. Optimum acidity of washing solution should be selected as 8 mol/L when the parameters were comprehensively considered.

3.4. Effect of acidity of desorption solution

The relationship between the concentration of iron and nickel and desorption solution is shown in Fig. 10. Fig. 11 shows the variation of cumulative elution rate of Fe(III) with volume of the feed solution. After the desorption, only

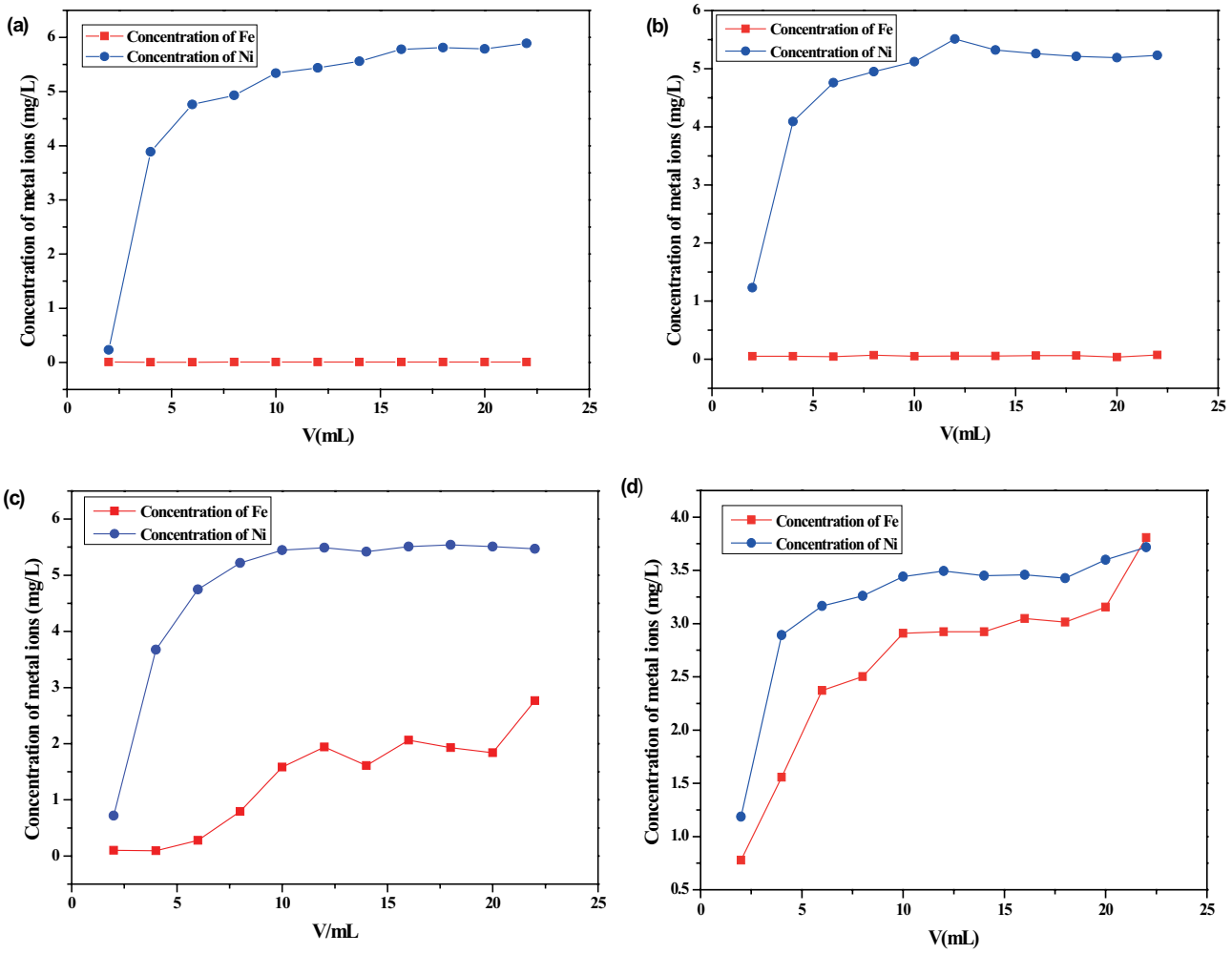

Fig. 5. The relationship between the concentration of iron and nickel with the effluent volume, (a) [H] = 8 mol/L, (b) [H] = 6 mol/L, (c) [H] = 4 mol/L, and (d) [H] = 2 mol/L. Conditions: T = 20°C; v = 0.5 mL/min; $V_{(feed\ solution)}$ = 22 mL.

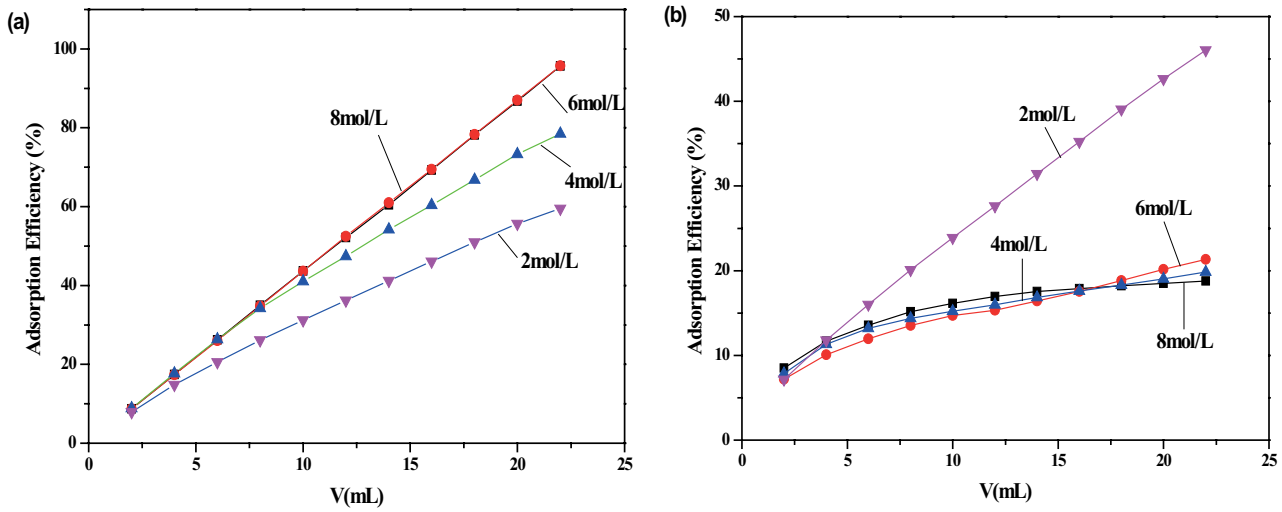

Fig. 6. Variation of cumulative adsorption rate with effluent volume: (a) variation of cumulative adsorption rate of Fe(III) with effluent volume and (b) variation of cumulative adsorption rate of Ni(II) with effluent volume. Conditions: T = 20°C; v = 0.5 mL/min; $V_{(\text{feed solution})}$ = 22 mL.

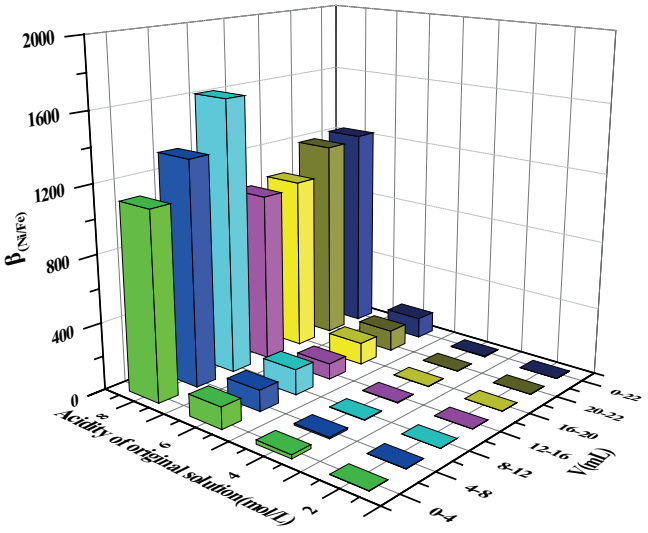

Fig. 7. Separation coefficients of Ni(II) and Fe(III) at different acidity of feed solution. Conditions: T = 20°C; v = 0.5 mL/min; $V_{(\text{feed solution})}$ = 22 mL.

a small amount of nickel existed in the desorption solution. A lot of iron, however, was eluted from the resin column. Meanwhile, at the initial stage of the desorption process, only a small amount of iron was eluted. When the volume of desorption solution was between 5 and 15 mL, a large amount of complex iron which was adsorbed by anion exchange resin was eluted. Under the condition of low acidity, iron will change from the complex state ($[FeCl_4]^-$ or $[FeCl_6]^{3-}$) to iron ion again and Fe^{3+} will be transferred to the eluate due to the weak adsorption capacity of anion resin to cation. This phenomenon can be explained by the following equations:

$$R-N(CH_3)_3[FeCl_4] = R-N(CH_3)_3Cl + Fe^{3+} + 3Cl^- \quad (11)$$

$$[R-N(CH_3)_3]_3[FeCl_6] = 3[R-N(CH_3)_3Cl] + Fe^{3+} + 3Cl^- \quad (12)$$

We also can get the following conclusion that the desorption efficiency of iron increased with the decrease of the acidity of the eluate. Meanwhile, When the concentration of hydrochloric acid decreased from 1 to 0.05 mol/L, The $\beta_{(Ni/Fe)}$ was also increasing gradually, which reached 1,120.39. Therefore, the acidity of 0.05 mol/L was selected as optimum.

3.5. Multiple adsorptions of anion resin under optimal conditions

From the above results, the optimal conditions of the separation method were determined to be as follows: The acidity of the feed solution, washing solution and desorption solution were chosen as 8, 8 and 0.05 mol/L, respectively. The volume of the feed solution, washing solution and desorption solution were chosen as 20, 10 and 20 mL, respectively. It was found that the adsorption performance of the anion resin did not decrease after five adsorption experiments from Fig. 12. The separation coefficients were more than 10^3, this means that 99.9% of Fe(III) and Ni(II) were successfully mutually separated.

In the past, many separation processes of Fe(III) and Ni(II) such as extraction, chemical precipitation, adsorption and ion exchange have been developed. Copper iron reagent, hydroxide and carbamate were used for precipitation–purification, but the recovery and decontamination factor was low. After that, new functional resins AG 50Wx8 resin [41–43], DGA resin [44,45], TEVA resin [46], TK400 [47], and UTEVA resin [48] were used. New functional materials such as fabrication of hierarchically porous metal alkylphosphonate framework [49] and new unsymmetrical diglycolamides etc [50] were also used to separate Fe-55 and Ni-63. Compared to these separation materials and methods, this modified separation method using nuclear anion resin (Model: ZG A NR 170)

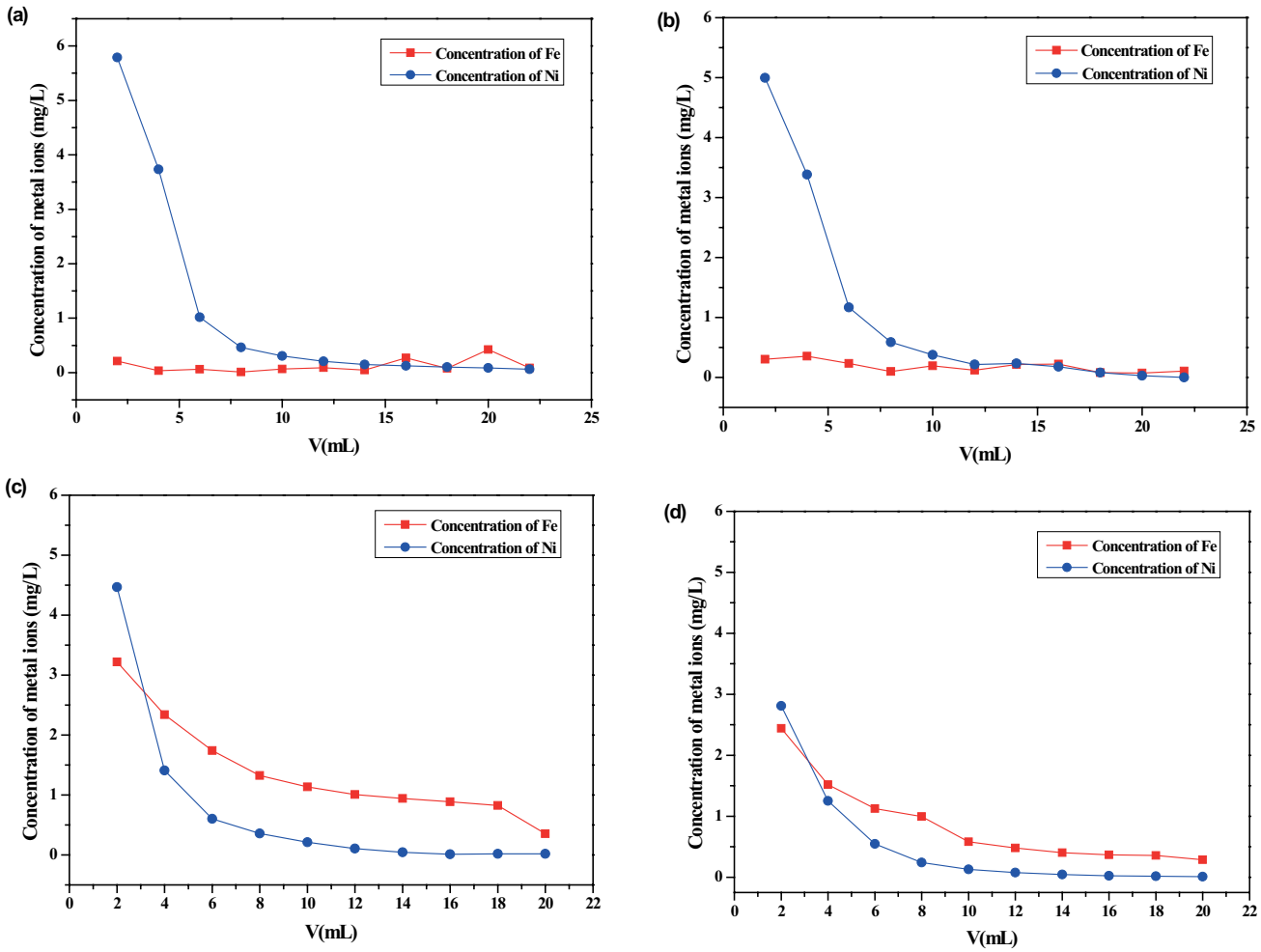

Fig. 8. The relationship between the concentration of iron and nickel in the volume of washing solution. (a) [H] = 8 mol/L, (b) [H] = 6 mol/L, (c) [H] = 4 mol/L, and (d) [H] = 2 mol/L. Conditions: T = 20°C; v = 0.5 mL/min; $V_{(\text{washing solution})}$ = 22 mL.

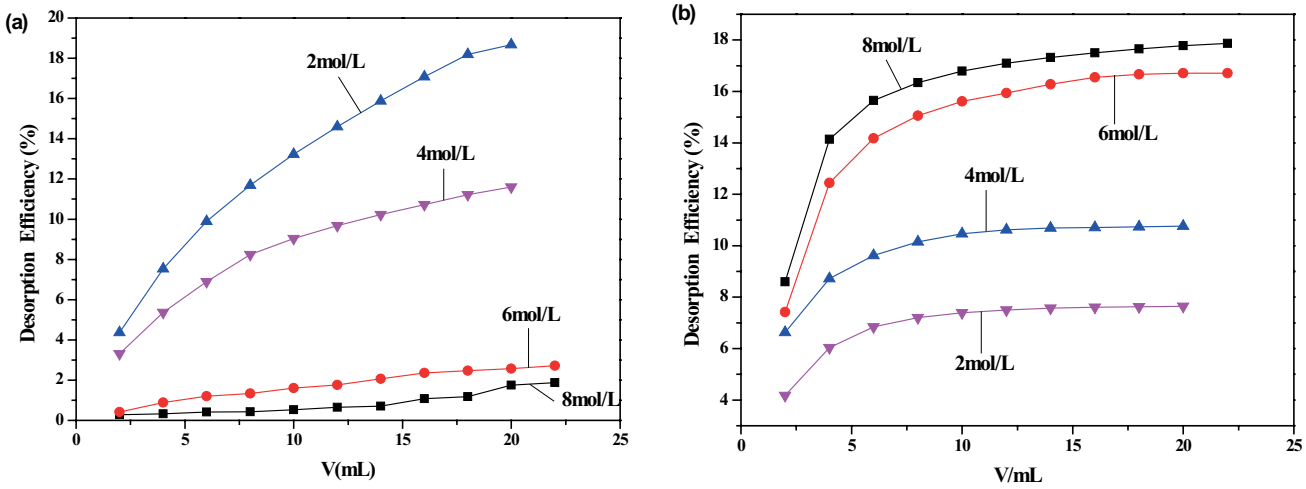

Fig. 9. Variation of cumulative desorption rate with the volume of washing solution: (a) variation of cumulative desorption rate of Fe(III) with the effluent volume of the feed solution and (b) variation of cumulative desorption rate of Ni(II) with the effluent volume of the feed solution. Conditions: T = 20°C; v = 0.5 mL/min; $V_{(\text{washing solution})}$ = 22 mL.

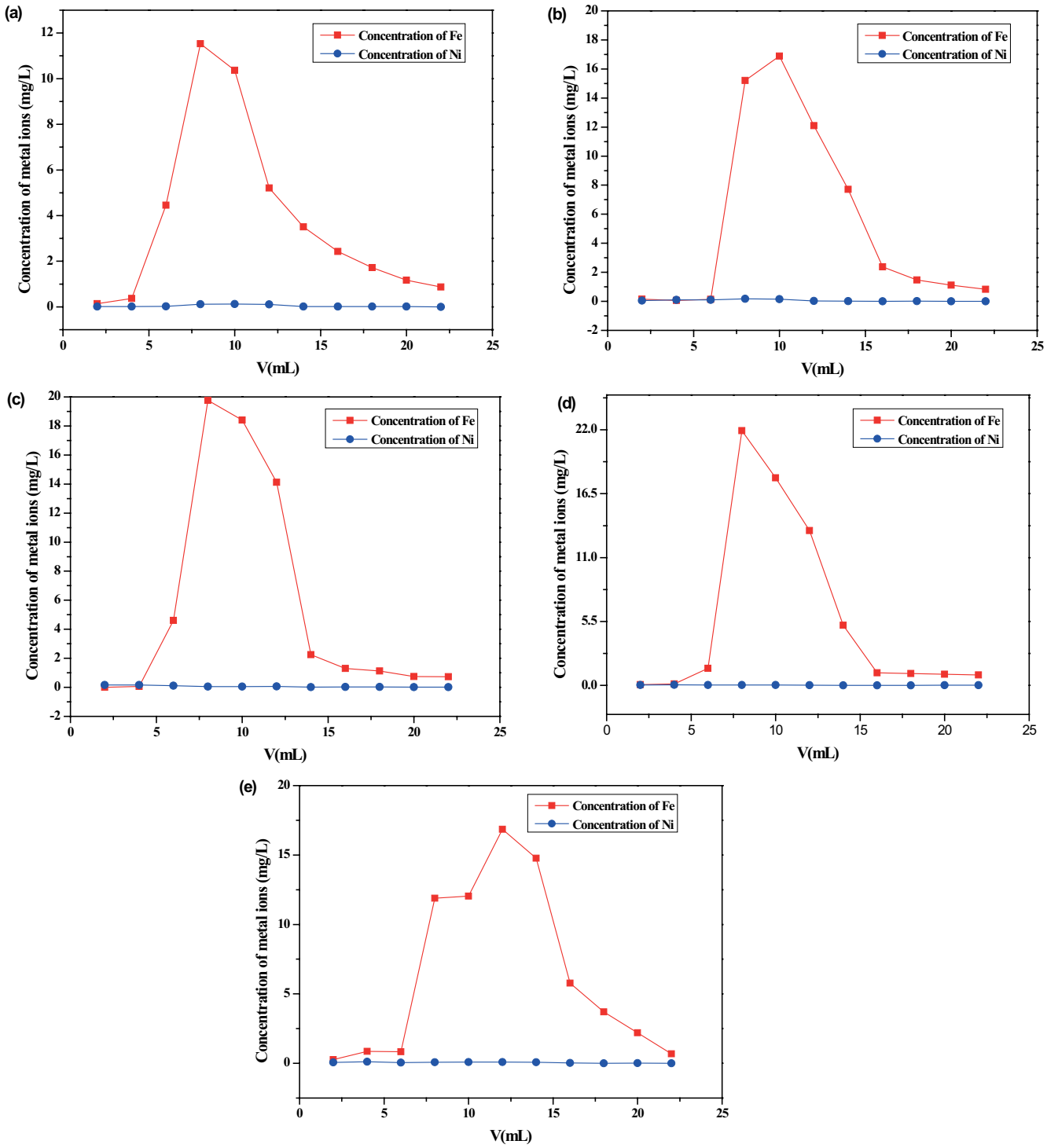

Fig. 10. The relationship between the concentration of Fe(III) and Ni(II) and volume of the desorption solution. (a) [H] = 1 mol/L, (b) [H] = 0.5 mol/L, (c) [H] = 0.25 mol/L, (d) [H] = 0.1 mol/L, and (e) [H] = 0.05 mol/L. Conditions: T = 20°C; v = 0.5 mL/min; $V_{(\text{desorption solution})}$ = 22 mL.

had good separation efficiency for sample matrix, low toxicity and chemical recovery. The nuclear grade resin had been proved to have good radiation resistance under real mixed irradiation field conditions, this was a fast, effective and economical method.

The separation method in this paper will be used in the purification of various complex systems such as stainless steel, zirconium alloy, burnable poison rod, fuel rod, APG resin in the next study. In view of the complexity of the above system, a new developing process with novel pretreatment

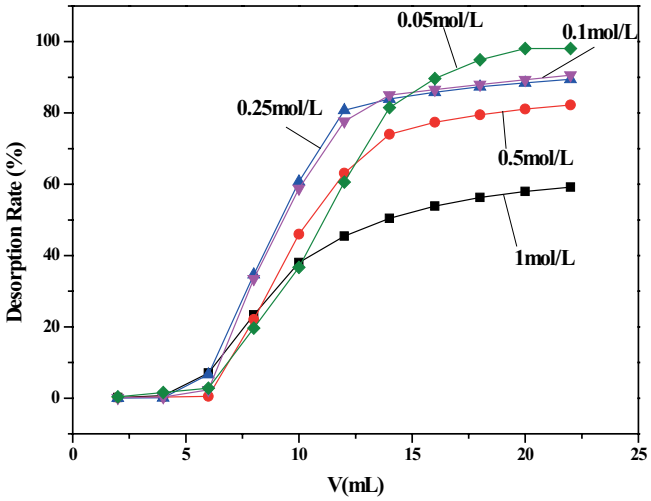

Fig. 11. Variation of cumulative elution rate of Fe(III) with volume of the feed solution. Conditions: T = 20°C; v = 0.5 mL/min; $V_{(\text{desorption solution})}$ = 22 mL.

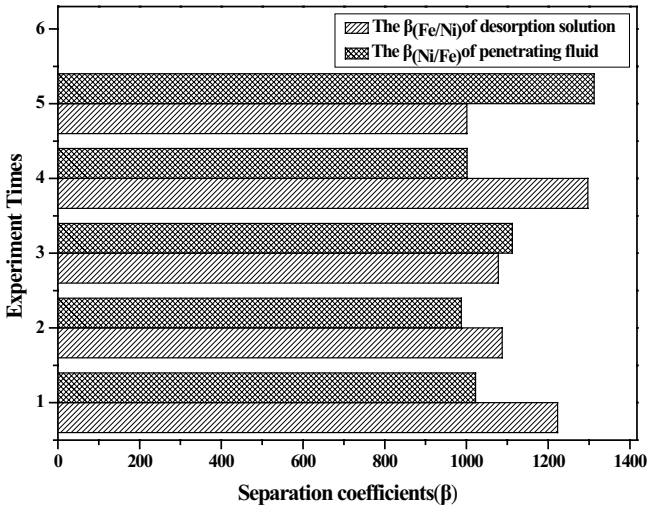

Fig. 12. The relationship between the separation coefficient and experiment times. Conditions: v = 0.5 mL/min; $C_{(\text{Fe})}$ = 6.63 ppm; $C_{(\text{Ni})}$ = 6.01 ppm.

technology and analysis methods such as advanced oxidation processes [51–53] is also the focus of our future work.

4. Conclusion

Separation experiments of Fe(III) and Ni(II) in radioactive wastewater simulation liquid were carried out by a novel nuclear anion resin and led to the following conclusions: (1) The optimal conditions for separate Fe(III) and Ni(II) from radioactive wastewater simulation liquid were found to be as follows: the acidity of the feed solution, washing solution and desorption solution were chosen as 8, 8 and 0.05 mol/L, respectively. The volume of the feed solution, washing solution and desorption solution were chosen as 20, 10 and 20 mL, respectively. (2) A very good separation effect could reach by ZG A NR 170 resin under optimal conditions. In the adsorption stage, more than 99% of iron could be adsorbed on the resin column, the $\beta_{(\text{Ni/Fe})}$ of penetrating fluid can reach 1,223.93. In the desorption process, the desorption rate of iron can be as high as 98%, the $\beta_{(\text{Fe/Ni})}$ of the desorption solution can reach 1,120.39. (3) The nuclear strong basic anion resin kept good performance, the volumetric mass-transfer coefficient of static adsorption process can reach 0.032 s^{-1} and it was found that the adsorption performance of the anion resin did not decrease after five adsorption experiments.

Acknowledgments

The authors gratefully acknowledge the support of the radiochemistry laboratory who funded this work and also acknowledge the helpful comments of other colleagues in the laboratory.

Symbols

C — Concentration of the main solution, kg/m^3
C_1 — Particle surface solution concentration, kg/m^3
C^* — Equilibrium concentration in equilibrium with adsorption quantity (q), kg/m^3
C_0 — Initial concentration with adsorbent, kg/m^3
C_e — Equilibrium concentration, kg/m^3
K_f^1 — Liquid membrane transfer coefficient, m/h
K_f — Total liquid membrane transfer coefficient, m/h
$K_f\alpha_v$ — Total liquid membrane volume mass transfer coefficient, h^{-1}
K_s^1 — Solid film transfer coefficient, m/h
K_s — Total solid film transfer coefficient, m/h
$K_s\alpha_v$ — Total solid film volume mass transfer coefficient, h^{-1}
m — Resin quality, kg
Q — Adsorption quantity, kg/kg
q^* — Adsorption quantity in equilibrium with concentration of the main solution (C), kg/kg
q_1 — Adsorption quantity in equilibrium with particle surface solution concentration, kg/kg
t — Absorption time or desorption time, min
V — Water sample volume, m^3
α_v — Outer area of the fill layer unit volume particles, m^2/m^3
ρ_b — Apparent density, kg/m^3

References

[1] Z. Majidnia, A. Idris, Evaluation of cesium removal from radioactive wastewater using maghemite PVA–alginate beads, Chem. Eng. J., 262 (2015) 372–382.
[2] G.E. McCullough, Concentration of radioactive liquid waste by evaporation, Ind. Eng. Chem., 43 (1951) 1505–1509.
[3] D.A. Reddy, S.K. Khandelwal, R. Muthiah, A.G. Shanmugamani, B. Paul, S.V.S. Rao, P.K. Sinha, Conditioning of sludge produced through chemical treatment of radioactive liquid waste – operating experiences, Ann. Nucl. Energy, 37 (2010) 934–941.
[4] C. Fortin, F. Caron, Complexing capacity of low-level radioactive waste leachates for ^{60}Co and ^{109}Cd using an ion-exchange technique, Anal. Chim. Acta, 410 (2000) 107–117.
[5] A.E. Osmanlioglu, Decontamination and solidification of liquid radioactive waste using natural zeolite, J. Mater. Cycles Waste Manage., 17 (2015) 690–694.

[6] A.E. Savkin, A.P. Varlakov, Development of a process for treatment and solidification of liquid radioactive concentrates from the Leipunskii Institute of Energy Physics, Radiochemistry, 53 (2011) 563–567.
[7] X.L. Hou, L.F. Østergaard, S.P. Nielsen, Determination of ^{63}Ni and ^{55}Fe in nuclear waste samples using radiochemical separation and liquid scintillation counting, Anal. Chim. Acta, 535 (2005) 297–307.
[8] X.L. Hou, Rapid analysis of ^{14}C and ^{3}H in graphite and concrete for decommissioning of nuclear reactor, Appl. Radiat. Isot., 62 (2005) 871–882.
[9] P. Povinec, The analysis of ^{3}H and ^{14}C labelled compounds in the form of doubly labelled methane, Int. J. Appl. Radiat. Isot., 26 (1975) 465–469.
[10] E. Gjeçi, Analysis of ^{90}Sr in environmental and biological samples by extraction chromatography using a crown ether, J. Radioanal. Nucl. Chem., 213 (1996) 165–174.
[11] S.J. Gomez, L.M.L. Valdivia, C.G. Iglesias, M.I. Rico Selas, Separation and concentration processes of solutions of Co(II), Ni(II), Cr(III), Fe(III) and Mn(II) by extraction with toluene-dissolved rosin, J. Chem. Technol. Biotechnol., 49 (1990) 267–274.
[12] X.M. Sun, J.R. Shen, G.Q. Zhan, B.H. Li, Continuous extraction and separation of Cu(II), Zn(II), Co(II), Ni(II) by using modified polymer affinity liquid-solid extraction system, Chin. J. Anal. Chem., 30 (2002) 218–221.
[13] H. Berber, G. Alpdogan, Solid phase extraction of trace Al(III), Fe(II), Co(II), Cu(II), Cd(II) and Pb(II) ions in beverages on functionalized polymer microspheres prior to flame atomic absorption spectrometric determinations, Anal. Sci., 33 (2017) 1427–1433.
[14] A. Fernandes, J.C. Afonso, A.J.B. Dutra, Separation of nickel(II), cobalt(II) and lanthanides from spent Ni-MH batteries by hydrochloric acid leaching, solvent extraction and precipitation, Hydrometallurgy, 133 (2013) 37–43.
[15] Y.-J. Shih, C.-P. Lin, Y.-H. Huang, Application of Fered-Fenton and chemical precipitation process for the treatment of electroless nickel plating wastewater, Sep. Purif. Technol., 104 (2013) 100–105.
[16] S. Tokalıoğlu, O. Daşdelen, Coprecipitation with Cu(II)-4-(2-pyridylazo)-resorcinol for separation and preconcentration of Fe(III) and Ni(II) in water and food samples, Clean—Soil Air Water, 39 (2011) 296–300.
[17] I.S.S. Pinto, S.M. Sadeghi, H.M.V.M. Soares, Separation and recovery of nickel, as a salt, from an EDTA leachate of spent hydrodesulphurization catalyst using precipitation methods, Chem. Eng. Sci., 122 (2015) 130–137.
[18] A. Yamakawa, K. Yamashita, A. Makishima, E. Nakamura, Chemical separation and mass spectrometry of Cr, Fe, Ni, Zn, and Cu in terrestrial and extraterrestrial materials using thermal ionization mass spectrometry, Anal. Chem., 81 (2009) 9787–9794.
[19] J. Liu, Z.F. Qiu, J. Yang, L.M. Cao, W. Zhang, Recovery of Mo and Ni from spent acrylonitrile catalysts using an oxidation leaching–chemical precipitation technique, Hydrometallurgy, 164 (2016) 64–70.
[20] P. Zhao, J. Jiang, F.-W. Zhang, W.-F. Zhao, J.-T. Liu, R. Li, Adsorption separation of Ni(II) ions by dialdehyde o-phenylenediamine starch from aqueous solution, Carbohydr. Polym., 81 (2010) 751–757.
[21] S.R. Shukla, R.S. Pai, A.D. Shendarkar, Adsorption of Ni(II), Zn(II) and Fe(II) on modified coir fibres, Sep. Purif. Technol., 47 (2006) 141–147.
[22] K.G. Bhattacharyya, S.S. Gupta, Adsorption of Fe(III), Co(II) and Ni(II) on ZrO–kaolinite and ZrO–montmorillonite surfaces in aqueous medium, Colloids Surf., A, 317 (2008) 71–79.
[23] M. Qureshi, H.S. Rathore, R. Kumar, Synthesis and ion-exchange properties of stannic arsenates: separation of Fe^{3+} from Ni^{2+}, CO^{2+}, Mn^{2+}, and Al^{3+}; Separation of Al^{3+} from Mg^{2+} and In^{2+}, J. Chem. Soc. A, 1970 (1986–1990), doi: 10.1039/J19700001986.
[24] K.S. Choi, C.H. Lee, H.J. Im, J.B. Yoo, H.J. Ahn, Separation of ^{99}Tc, ^{90}Sr, ^{59}Fe, ^{63}Ni, ^{55}Fe and ^{94}Nb from activated carbon and stainless steel waste samples, J. Radioanal. Nucl. Chem., 314 (2017) 2145–2154.
[25] N. Muslu, M. Gülfen, Selective separation and concentration of Pd(II) from Fe(III), Co(II), Ni(II), and Cu(II) ions using thiourea-formaldehyde resin, J. Appl. Polym. Sci., 120 (2011) 3316–3324.
[26] R.-S. Juang, Y.-C. Wang, Use of complexing agents for effective ion-exchange separation of Co(II)/Ni(II) from aqueous solutions, Water Res., 37 (2003) 845–852.
[27] M.A.R. Ahamed, R. Subha, D. Jeyakumar, A.R. Burkanudeen, Separation of metal ions by the influence of a cation-exchange terpolymer involving 2-amino-6-nitrobenzothiazole-ethylenediamine-formaldehyde, Polym. Int., 64 (2015) 126–137.
[28] M.F. Bari, M.S. Hossain, I.M. Mujtaba, S.B. Jamaluddin, K. Hussin, Simultaneous extraction and separation of Cu(II), Zn(II), Fe(III) and Ni(II) by polystyrene microcapsules coated with Cyanex 272, Hydrometallurgy, 95 (2009) 308–315.
[29] Q. Dong, Separation of nickel, cobalt and copper by solvent extraction with P204, J. China Nonferrous Met. Soc., 11 (2001) 803–805.
[30] L.J. Song, L. Ma, Y. Ma, Y.G. Yang, X.X. Dai, Method for sequential determination of ^{55}Fe and ^{63}Ni in leaching solution from cement solidification, J. Radioanal. Nucl. Chem., 319 (2019) 1227–1234.
[31] D. Kogelnig, A. Stojanovic, F. Jirsa, W. Körner, R. Krachler, B.K. Keppler, Transport and separation of iron(III) from nickel(II) with the ionic liquid trihexyl(tetradecyl)phosphonium chloride, Sep. Purif. Technol., 72 (2010) 56–60.
[32] M.N. Kashid, A. Renken, L. Kiwi-Minsker, Gas–liquid and liquid–liquid mass transfer in micro-structured reactors, Chem. Eng. Sci., 66 (2011) 3876–3897.
[33] A. Ghaini, M.N. Kashid, D.W. Agar, Effective interfacial area for mass transfer in the liquid–liquid slug flow capillary microreactors, Chem. Eng. Process., 49 (2010) 358–366.
[34] J. Haber, B. Jiang, T. Maeder, N. Borhani, J. Thome, A. Renken, L. Kiwi-Minsker, Intensification of highly exothermic fast reaction by multi-injection microstructured reactor, Chem. Eng. Process., 84 (2014) 14–23.
[35] A. Renken, V. Hessel, P. Löb, R. Miszczuk, M. Uerdingen, L. Kiwi-Minsker, Ionic liquid synthesis in a micro-structured reactor for process intensification, Chem. Eng. Process., 46 (2007) 840–845.
[36] D.A. Waterkamp, M. Heiland, M. Schlüter, J.C. Sauvageau, T. Beyersdorff, J. Thöming, Synthesis of ionic liquids in micro-reactors—a process intensification study, Green Chem., 9 (2007) 1084–1089.
[37] N. Sen, K.K. Singh, S. Mukhopadhyay, K.T. Shenoy, S.K. Ghosh, Continuous, solvent free, high temperature synthesis of ionic liquid 1-butyl-3-methylimidazolium bromide in a microreactor, BARC Newsl., 334 (2013) 20–23.
[38] G. Veser, Experimental and theoretical investigation of H_2 oxidation in a high-temperature catalytic microreactor, Chem. Eng. Sci., 56 (2001) 1265–1273.
[39] P.E. Warwick, I.W. Croudace, Isolation and quantification of ^{55}Fe and ^{63}Ni in reactor effluents using extraction chromatography and liquid scintillation analysis, Anal. Chim. Acta, 567 (2006) 277–285.
[40] C.A. Nogueira, P.C. Oliveira, F.M. Pedrosa, Separation of cadmium, cobalt, and nickel by solvent extraction using the nickel salts of the extractants, Solvent Extr. Ion Exch., 27 (2009) 295–311.
[41] C.-K. Kim, M.H. Lee, P. Martin, Method validation of a procedure for determination of ^{210}Po in water using DDTC solvent extraction and Sr resin, J. Radioanal. Nucl. Chem., 279 (2009) 639–646.
[42] P. Pichestapong, W. Sriwiang, U. Injarean, Separation of Yttrium-90 from Strontium-90 by extraction chromatography using combined Sr resin and RE resin, Energy Procedia, 89 (2016) 366–372.
[43] K.N. Kmak, J.D. Despotopulos, D.A. Shaughnessy, Separation of Pb, Bi and Po by cation exchange resin, J. Radioanal. Nucl. Chem., 314 (2017) 985–989.
[44] Z. Kazi, N. Guérin, M. Christl, M. Totland, A. Gagné, S. Burrell, Effective separation of Am(III) and Cm(III) using a DGA resin

via the selective oxidation of Am(III) to Am(V), J. Radioanal. Nucl. Chem., 321 (2019) 227–233.
[45] D. Arginelli, P. Battisti, I. Giardina, Extraction chromatography with DGA resin for the determination of americium and curium in biological samples by high resolution alpha spectrometry, J. Radioanal. Nucl. Chem., 309 (2016) 279–284.
[46] K. Kołacińska, Z. Samczyński, J. Dudek, A. Bojanowska-Czajka, M. Trojanowicz, A comparison study on the use of Dowex1 and TEVA-resin in determination of ^{99}Tc in environmental and nuclear coolant samples in a SIA system with ICP-MS detection, Talanta, 184 (2018) 527–536.
[47] F. Sufke, J. Lippold, S. Happel, Improved separation of Pa from Th and U in marine sediments with TK400 resin, Anal. Chem., 90 (2018) 1395–1401.
[48] M. Skinner, D. Knight, The behaviour of selected fission products and actinides on UTEVA® resin, J. Radioanal. Nucl. Chem., 307 (2016) 2549–2555.
[49] X.J. Peng, J.X. Han, G.Z. Yuan, J.L. Zhao, Y. Cui, G.X. Sun, Separation of Pr(III) and Fe(III) by unsymmetrical diglycolamides from nitric acid media, Sep. Purif. Technol., 217 (2019) 294–298.
[50] K. Lv, C.-T. Yang, Y. Liu, S. Hu, X-L. Wang, The hydrolytic stability and degradation mechanism of a hierarchically porous metal alkylphosphonate framework, Nanomaterials, 8 (2018) 166–181.
[51] M. Moradi, Y. Vasseghian, A. Khataee, M. Kobya, H. Arabzade, E.-N. Dragoi, Service life and stability of electrodes applied in electrochemical advanced oxidation processes: a comprehensive review, J. Ind. Eng. Chem., 87 (2020) 18–39.
[52] M. Moradi, A. Elahinia, Y. Vasseghian, E.-N. Dragoi, F. Omidi, A.M. Khaneghah, A review on pollutants removal by Sono-photo-Fenton processes, J. Ind. Eng. Chem., 8 (2020) 104330–104349.
[53] M. Moradi, Y. Vasseghian, H. Arabzade, A.M. Khaneghah, Various wastewaters treatment by sono-electrocoagulation process: a comprehensive review of operational parameters and future outlook, Chemosphere, 263 (2020) 128314–128334.